CHINESE JOURNAL OF PHYSICS VOL. 37, NO. 4 AUGUST 1999

Quantum Transport in a Double-Barrier Structure in the Presence of a Finite-Range Time-Modulated Potential

C. S. Chu and H. C. Liang

Department of Electrophysics, National Chiao Tung University, *Hsinchu, Taiwan 300, Taiwan, R.O.C.*

(Received November 2, **1998;** revised manuscript received December 3, 1998)

We have studied the quantum transport phenomena in a double-barrier structure acted upon by a finite-range time-modulated potential. Inter-side-band $m\hbar\omega$ transitions are made possible by the finiteness in the range of the oscillating field. For the case when the barrier width is small, such that the resonance state in between the barriers is too broadened, the dc conductance G exhibits peaks or dip structures when the chemical potential μ is at $m\hbar\omega$ above the band bottom. For the case when the barrier width is large, such that the resonance state in between the barriers is well defined, the above feature is masked by resonant tunneling processes when μ is at energies mhw away from the resonant energy E_b. In both cases, the dips or peaks in G are due to the temporary trapping of the transmitting electrons by the quasi-bound states. Furthermore, for the latter case, we also obtain the quenching of the resonant transmission found by Wagner, but with a small quantitative modification. Our calculation is nonperturbative which is valid for arbitrary potential strength and frequency. The form of the time-modulated potential is expected to be realized in a gate-induced potential configuration.

PACS. 72.10.-d – Theory of electronic transport; scattering mechanisms
PACS. 72.40.+w – Photoconduction and photovoltaic effects.
PACS. 73.40.-c – Electronic transport in interface structures.

I. Introduction

Inelastic scattering processes in quantum transport have drawn continued attention in the recent past. These studies have demonstrated, among others, the interesting feedback effect of the inelastic scattering on the elastic channel. One of the common models used is a time-modulated potential that has a finite spatial profile [1-11]. This model for the coherent inelastic scattering can be realized in the case when the time-modulated potential is well specified.

The coherent inelastic scattering processes are expected to manifest in nanostructures such as a gate-controlled double-barrier structure, as shown in Fig. 1. Similar configuration has been considered recently by Wagner [7,8], who has studied the transmission coefficients of a well acted upon by an oscillating potential. Focusing on the resonant tunneling through the double barrier, he found the quenching conditions for each side-band, when the emanating electron has an energy change of $m\hbar\omega$. In this work, however, we perform a comprehensive investigation of the transport characteristics in the double-barrier structure. A simple mode-matching method is utilized. This method is nonperturbative, and allows both the frequency and the amplitude of the oscillating potential to have arbitrary values.

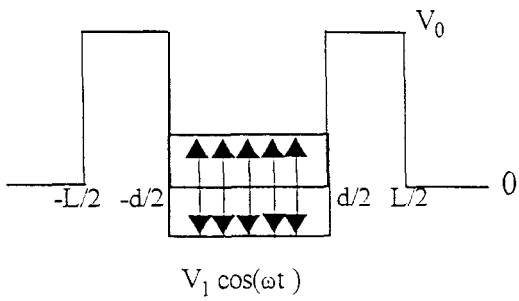

FIG. 1. Sketch of a double-barrier structure with a time-modulated potential in between the barriers. The oscillating potential gives rise to intra-band and inter-side-band transitions.

In reference [11], dip structures are found in the dc conductance G when narrow constrictions are acted upon by a time-modulated potential. These dip structures are closely related to the density of states (DOS). In fact, the dip structures are the quasi-bound-state features, which occur when the electrons can make transitions to the quasi-bound-states formed just below a subband bottom by giving away $m\hbar\omega$. The existence of these quasi-bound states is closely associated with the singular DOS at a subband bottom. We have also studied the transport characteristics of a quantum well with a time-modulated potential in the well [12]. The quasi-bound-state features are found in G when μ is at energies mhw above the bound state energy in the well. Thus it is interesting to explore the manifestation of such quasi-bound-state features in a double-barrier structure. The extent of the quasi-boundedness for the resonant states formed between the double-barrier is very sensitive to both the height and the thickness of the barriers. In the neighborhood of a loosely bound level the effective DOS changes gradually, thus we expect to have weak side-band resonances. In the neighborhood of a tightly bound level, when the effective DOS changes abruptly, we expect to have strong side-band resonances. This feature is supported by the numerical results in this paper. There is, however, another set of side-band resonances. which occur when μ is at $m\hbar\omega$ above the energy bottom of the system. This set of side-band resonances is found to dominate in the case of the loosely bound levels, and is suppressed in the case of the tightly bound levels.

The configuration we consider in this work is a double-barrier structure with a time-modulated potential $V_1 \cos(\omega t)$ acting upon the region between the two barriers. The configuration is shown in Fig. 1. The finiteness in the range of the time-modulated potential alone gives rise to the following important consequences. First, the potential breaks the translational invariance, thus allowing the intra-band and inter-side-band transitions to occur for the transmitting electrons. Second, the reservoirs at both ends of the system are free from the time-modulation effects so that the distribution of the incident electrons is well determined. Thus the quantum transport can be casted into a Landauer-Biittiker-type formalism. Third, when the range L of the time-modulated potential is less than the phase-breaking length l_ϕ, the entire transmission process becomes coherent and can be described by a time-dependent Schrödinger equation. Within the recent experimental capabilities. 1, can be made sufficiently long by lowering the temperature.

In Sec. II we present the formulation for the inelastic scattering and express the conductance G in terms of the current transmission coefficients. In Sec. III we present numerical examples illustrating the quasi-bound features in G. Finally, Sec. IV presents a conclusion.

II. Theory

In this section, the inelastic scattering problem is formulated and the equations for the current transmission and the current reflection coefficients are obtained. Conductance G is then expressed in terms of these coefficients. The potential takes the form

$$V(x,t) = V_0\theta(|x|-d/2)\theta(L/2-|x|) + V_1\cos(\omega t)\theta(d/2-|x|), \tag{1}$$

where V_0 is the barrier height, $\frac{L-d}{2}$ is the barrier thickness, and d is the distance between the barriers. Choosing the energy unit $E^*=\hbar^2k_F^2/2m^*$, the length unit $a^*=1/k_F$, the time unit $t^*=\hbar/E^*$, V_0 and V_1 in units of E^*, we obtain the dimensionless Schrödinger equation, given by

$$\left[-\frac{\partial^2}{\partial x^2}+V(x,t)\right]\Psi(x,t)=i\frac{\partial}{\partial t}\Psi(x,t). \tag{2}$$

Here k_F is a typical Fermi wave vector of the reservoir and m^* is the effective mass. For an electron incident from the left electrode and at energy μ, the scattering wave function can be written in the form [7, 11, 12]

$$\Psi(x,t)=\begin{cases} e^{ik_0(x+\frac{L}{2})}e^{-i\mu t}+\sum_m r_m e^{-ik_m(x+\frac{L}{2})}e^{-i(\mu+m\omega)t} & \text{if } x < -L/2 \\ \sum_m [A_m^l e^{iq_m(x+\frac{L}{2})}+B_m^l e^{-iq_m(x+\frac{L}{2})}]e^{-i(\mu+m\omega)t} & \text{if } -L/2 < x < -d/2 \\ \sum_{m'}[J_{m'}(V_1/\omega)e^{-im'\omega t}]\sum_m [C_m e^{ik_m x}+D_m e^{-ik_m x}]e^{-i(\mu+m\omega)t} & \text{if } -d/2 < x < d/2 \\ \sum_m [A_m^r e^{-iq_m(x-\frac{L}{2})}+B_m^r e^{iq_m(x-\frac{L}{2})}]e^{-i(\mu+m\omega)t} & \text{if } d/2 < x < L/2 \\ \sum_m t_m e^{ik_m(x-\frac{L}{2})}e^{-i(\mu+m\omega)t}, & \text{if } x > L/2 \end{cases} \tag{3}$$

where m, m' are the sideband indices which run through all integer numbers. These sideband indices m denote the net energy change $m\hbar\omega$ in the emanating electrons. The effective wave vector for an electron with energy ε is given by $q_m=\sqrt{\varepsilon-V_0+mw}$ in the barrier region and $k_m=\sqrt{\varepsilon+m\omega}$ outside the barrier region.

The current reflection and the current transmission coefficients can be obtained from matching the wave functions, and their derivatives, at the four edges of the barriers and at all time. Thus from the matching at $x=\pm L/2$, we obtain

$$B_m^l = [A_m^l(q_m+k_m)-2\delta_{m,0}k_m]/[q_m-k_m], \tag{4}$$

$$r_m = [2A_m^l q_m - \delta_{m,0}(q_m + k_m)]/[q_m - k_m], \tag{5}$$

$$B_m^r = A_m^r(q_m + k_m)/[q_m - k_m], \tag{6}$$

$$t_m = 2A_m^r q_m/[q_m - k_m]. \tag{7}$$

After performing the matching at $x = -d/2$, we obtain

$$\begin{aligned} &A_m^l\left[e^{iq_m\frac{L-d}{2}} + e^{-iq_m\frac{L-d}{2}}\frac{(q_m+k_m)}{(q_m-k_m)}\right] - 2\delta_{m,0}\frac{k_m e^{-iq_m\frac{L-d}{2}}}{(q_m-k_m)} \\ &= \sum_n \left[C_n e^{-ik_n\frac{d}{2}} + D_n e^{ik_n\frac{d}{2}}\right] J_{m-n}\left(\frac{V_1}{\omega}\right), \end{aligned} \tag{8}$$

$$\begin{aligned} &A_m^l\left[e^{iq_m\frac{L-d}{2}} + e^{-iq_m\frac{L-d}{2}}\frac{(q_m+k_m)}{(q_m-k_m)}\right] + 2\delta_{m,0}\frac{k_m e^{-iq_m\frac{L-d}{2}}}{(q_m-k_m)} \\ &= \sum_n \frac{k_n}{q_m}\left[C_n e^{-ik_n\frac{d}{2}} + D_n e^{ik_n\frac{d}{2}}\right] J_{m-n}\left(\frac{V_1}{\omega}\right), \end{aligned} \tag{9}$$

After performing the matching at $x = d/2$, we obtain

$$\begin{aligned} &A_m^r\left[e^{-iq_m\frac{d-L}{2}} + e^{iq_m\frac{d-L}{2}}\frac{(q_m+k_m)}{(q_m-k_m)}\right] \\ &= \sum_n \left[C_n e^{ik_n\frac{d}{2}} + D_n e^{-ik_n\frac{d}{2}}\right] J_{m-n}\left(\frac{V_1}{\omega}\right), \end{aligned} \tag{10}$$

$$\begin{aligned} &A_m^r\left[-e^{-iq_m\frac{d-L}{2}} + e^{iq_m\frac{d-L}{2}}\frac{(q_m+k_m)}{(q_m-k_m)}\right] \\ &= \sum_n \frac{k_n}{q_m}\left[C_n e^{ik_n\frac{d}{2}} - D_n e^{-ik_n\frac{d}{2}}\right] J_{m-n}\left(\frac{V_1}{\omega}\right). \end{aligned} \tag{11}$$

The zero-temperature conductance G is given by

$$G = \sum_m G(m) = \frac{2e^2}{h}\sum_m \frac{k_m}{k_0}|t_m|^2, \tag{12}$$

where m includes only propagating modes whose k_m is real. The factor of 2 is due to the spin degeneracy. Solving Eqs. (8)-(11), we obtain A_m^l, A_m^r, C_m, and D_m. We then obtain r_m and t_m by Eqs. (5) and (7).

We solve the coefficients r_m and t_m exactly, in the numerical sense, by imposing a large enough cutoff to the side-band index m. The correctness of our procedure is checked by the conservation of current condition, given by

$$\sum_m \frac{k_m}{k_0}[|r_m|^2 + |t_m|^2] = 1, \tag{13}$$

where m includes again only propagating modes with real k_m, and is also checked by the convergence of our results with the cutoff side-band index.

III. Numerical results

In this section, the transport characteristics of G in a double-barrier structure due to the presence of a time-modulated potential are presented. Before we present our numerical results, it is helpful to mention two types of multiple scattering processes that could occur within the structure. The first one is the multiple scattering between the two inner edges of the two barriers. A resonance in this multiple scattering process will give the true bound states, if the outer edges of the two barriers are very far away, or will give the resonant levels if the outer edges of the barriers are not very far away. The condition for the true bound states that have even parity is given by

$$\tan\left[\frac{d}{2}\sqrt{V_0 F}\right] - \frac{\sqrt{1-F}}{\sqrt{F}} = 0; \tag{14}$$

where, for the odd-parity bound states, it is

$$\tan\left[\frac{d}{2}\sqrt{V_0 F}\right] + \frac{\sqrt{F}}{\sqrt{1-F}} = 0. \tag{15}$$

Here $F = E_b/V_0$. The second type of multiple scattering process is the multiple scattering between the two outer edges of the two barriers. The resonant condition for this multiple scattering process is $2[q_0(L-d) + k_0 d] = 2n\pi$. This condition can be written in terms of the corresponding electron energy, which we will refer to as the harmonic energy E_n^h, given by

$$(L-d)\sqrt{2m^*(E_n^h - V_0)} + d\sqrt{E_n^h} = n\pi\hbar. \tag{16}$$

These two types of multiple scattering processes compete between themselves before they can manifest in the transport characteristics of G. In the following, we present G versus μ and its dependence on the structure parameters L, d, V_0, V_1, and ω. We first present, in Figs. 2(a-c), the dependence of the $G(\mu)$ relation on L when the time-modulated potential is not applied ($V_1 = 0$). Then, in Figs. 3(a-c), the dependence of the $G(\mu)$ relation on L is presented when the time-modulated potential is applied. The dependence of the $G(\mu)$ relation on ω is presented in Figs. 4(a,b). The dependence of the $G(\mu)$ relation on V_1 is presented in Figs. 5(a-c). Finally, in Figs. 6(a,b), $G(m)$ is plotted against V_1/ω. Figures 5 and 6 provide a comparison with the results of Wagner [7].

In our numerical examples, we choose an energy unit $E^* = \hbar^2 k_F^2/(2m^*) = 9$ meV, a length unit $a^* = 1/k_F = 79.6$ Å, and a frequency unit $\omega^* = E^*/\hbar = 13.6$ THz.

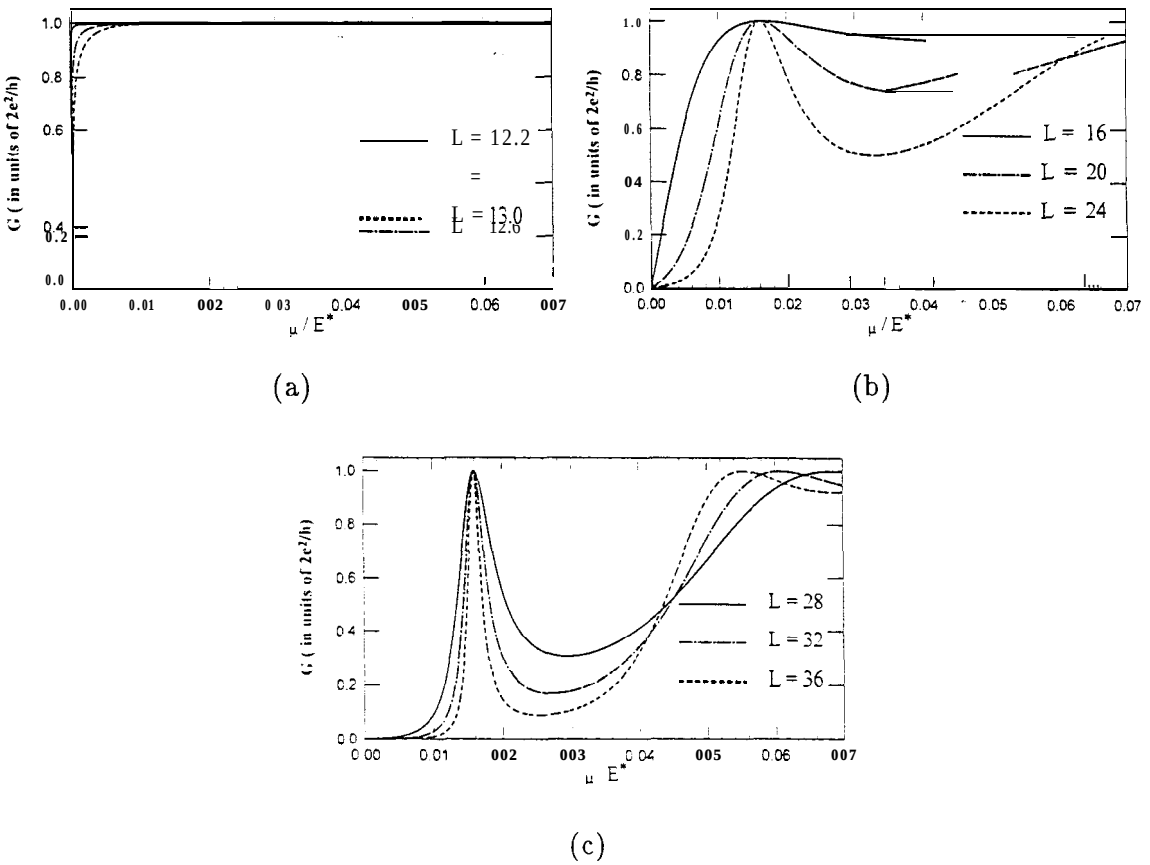

FIG. 2. Conductance G as a function of μ for a double-barrier structure. Well width $d = 12$, barrier height $V_0 = 0.03$, and L = 12.2, 12.6, 13.0 in (a), 16, 20, 24 in (b), and 28, 32, 36 in (c). The resonant transmission peak is sharper and is very close to $E_b = 0.0159$. The other shallower peak in Fig. 2(c) corresponds very closely to the $n = 2$ harmonics E_2^h.

In Figs. 2(a-c), $d = 12$, $V_0 = 0.03$, $V_1 = 0$, and L = 12.2, 12.6, 13.0 in (a); 16. 20, 24 in (b); and 28, 32, 36 in (c). The configuration allows only one resonant state, at $E_b = 0.015879$. The resonant transmission does not appear in G when the barrier thickness is small, as shown in Fig. 2(a), when the resonant level becomes too broadened. In Figs. 2(b) and (c), the resonant transmission peak in G becomes narrower as L increases. The location of the peak is at E_b. The n = 2 harmonics are at E_2^h = 0.069, 0.059, and 0.052, for L = 28, 32, 36, respectively, as shown in Fig. 2(c).

In Figs. 3(a-c), $d = 12$, V_0 = 0.03, w = 0.014, V_1 = 0.012, and the lengths L are the same as in Figs. 2(a-c). When the resonant level is too broadened, as in Fig. 3(a), the dip or peak structures in G are at $\mu = m\hbar\omega$. These are the quasi-bound-state features because the electrons can emit $m\hbar\omega$ and make transitions to the quasi-bound-state just below the band bottom. As the length L, or the barrier thickness, increases the resonant transmission structure starts to show up. These new peaks in G are at $\mu = E_b \pm m\hbar\omega$, and the peaks

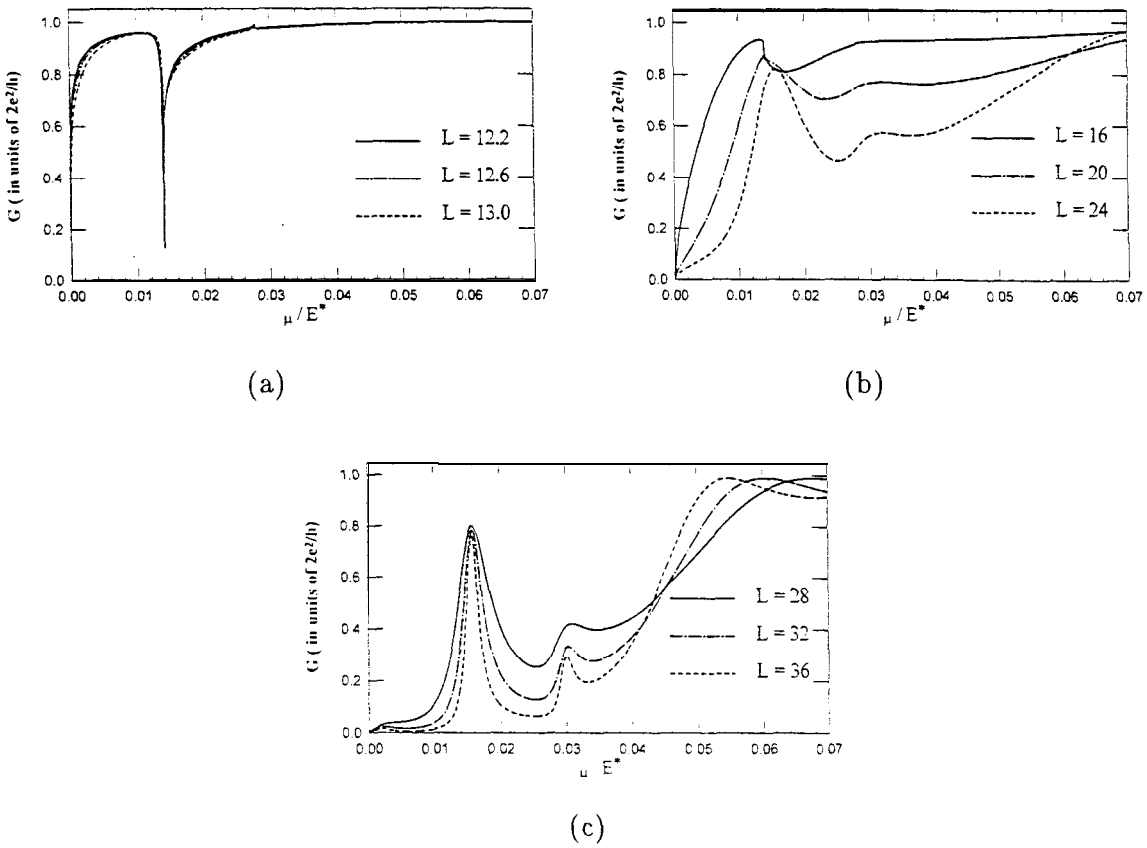

FIG. 3. Conductance G as a function of μ for a double-barrier structure acted upon by a time-modulated potential. Well width d = 12, barrier height V_0 = 0.03, $V_1 = 0.012$, and w = 0.014. The lengths L are the same as in Figs. 2(a-c). Fig. 3(a) shows that when the resonant states are too broadened to show up in G, the dip or peak structures in G occur at $\mu = m\hbar\omega$. Fig. 3(c) shows that when the resonant states are well defined, resonant transmission occurs near $\mu = E_b \pm m\hbar\omega$, and the harmonic peaks occur as well. Fig. 3(b) shows the crossover of all these structures in G for intermediate values of L.

are narrower for larger L, as shown in Fig. 3(c). These peaks correspond to situations when the electrons emit or absorb m photons and make transitions to the resonant level. The harmonic structures in G are clearly shown in Fig. 3(c).

In Figs. 4(a,b), $d = 12$, V_0 = 0.03, V_1 = 0.012, and w = 0.012, 0.015, 0.018. Fig. 4(a) is for $L = 13$, when the resonant level is very broadened, and Fig. 4(b) is for $L = 36$ when the resonant level is well defined. Fig. 4(a) shows the quasi-bound-state features at $\mu = m\hbar\omega$. Fig. 4(b) shows the set of resonance transmissions at $\mu = E_b \pm m\hbar\omega$. It is clear then that the quasi-bound-state features occur at the thin barrier regime, whereas the resonance transmission features dominate in the thick barrier regime.

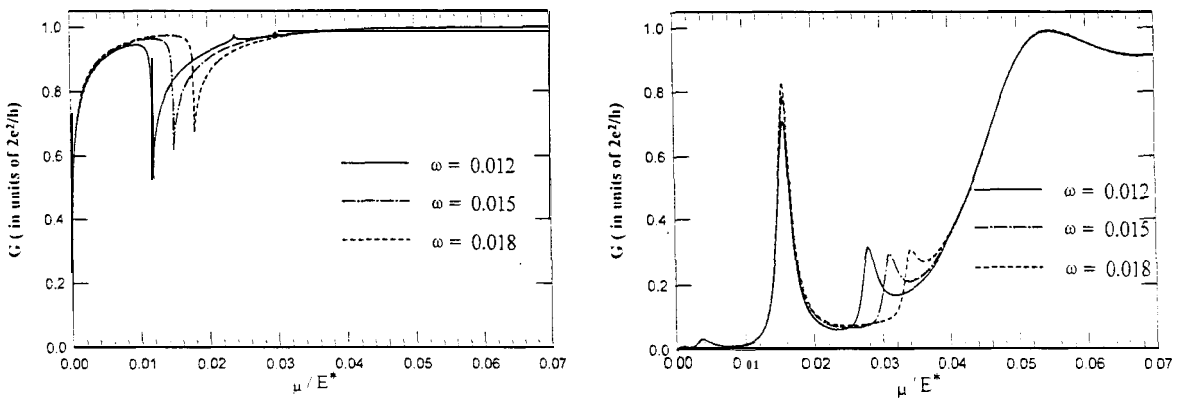

FIG. 4. Conductance G as a function of μ for a double-barrier structure acted upon by a time-modulated potential. Well width d = 12, barrier height V_0 = 0.03, and V_1 = 0.012. In Fig. 4(a), L = 13, and ω = 0.012, 0.015, and 0.018. The dip or peak structures in G are at $\mu = m\hbar\omega$. In Fig. 4(b), L = 36, and ω = 0.012, 0.015, and 0.018. The resonant transmission structures are at $\mu = E_b \pm m\hbar\omega$.

In the following, we try to make connection with the work of Wagner [7], who considered the case when $\hbar\omega$ is less than the energy width of the resonance transmission peak. For a direct comparison with the Fig. 4 in reference [7], we choose d = 50/79.6, $L = 3d$. $V_0 = 500/9$, and $\omega = 0.014$. With this choice of the structure parameters, there is one even parity resonance level, at E_b^e = 11.99, and one odd parity resonance level, at E_b^o = 43.1.

In Fig. 5(a), V_1 = 0.03, the time-modulated potential is too weak to induce photon-assisted transmissions in the neighborhood of the two resonance levels. Only two $\mu = E_b^{e(o)}$ peaks are found while the even parity resonance peak is much sharper. But in Fig. 5(b). when $V_1 = 2.585\omega$ is of a value slightly larger than that in Fig. 5(a), it induces a series of quenching structures to the resonant transmission peak of the sharper resonance level, at $\mu = E_b^e$. The condition for the occurrence of these quenching structures is that the ratio V_1/ω equals a root of the Bessel function $J_0(x)$[7]. These quenching structures are separated by an energy of about ω, as predicted by Wagner [7]. There is, however, no such quenching to the resonant transmission peak at E_b^o = 43.1, as shown in Fig. 5(c). We have investigated a bit further by lowering the barrier height to $V_0 = 50/9$, such that there is only one resonant state. The quenching effect is also not found in the neighborhood of the resonant level. Our results thus demonstrate that the quenching effect occurs for sufficiently sharp resonance transmission peak.

In Figs. 6(a,b), d = 50/79.6, $L = 3d$, $V_0 = 500/9$, and $\omega = 0.014$. We plot in Fig. 6(a) the conductance components G(m) against V_1/ω at the peak of the first resonance transmission where μ = 11.99. We find that G(m) = G(-m). But if we plot G(m) against V_1/ω at $\mu = E_b$ = 11.992, we find that G(m) is not symmetric with respect to m = 0. as shown in Fig. 6(b). The discrepancy is due to the shifting in the resonant level due to the finite thickness in the barrier and to the effect of the time-modulated potential. Our result

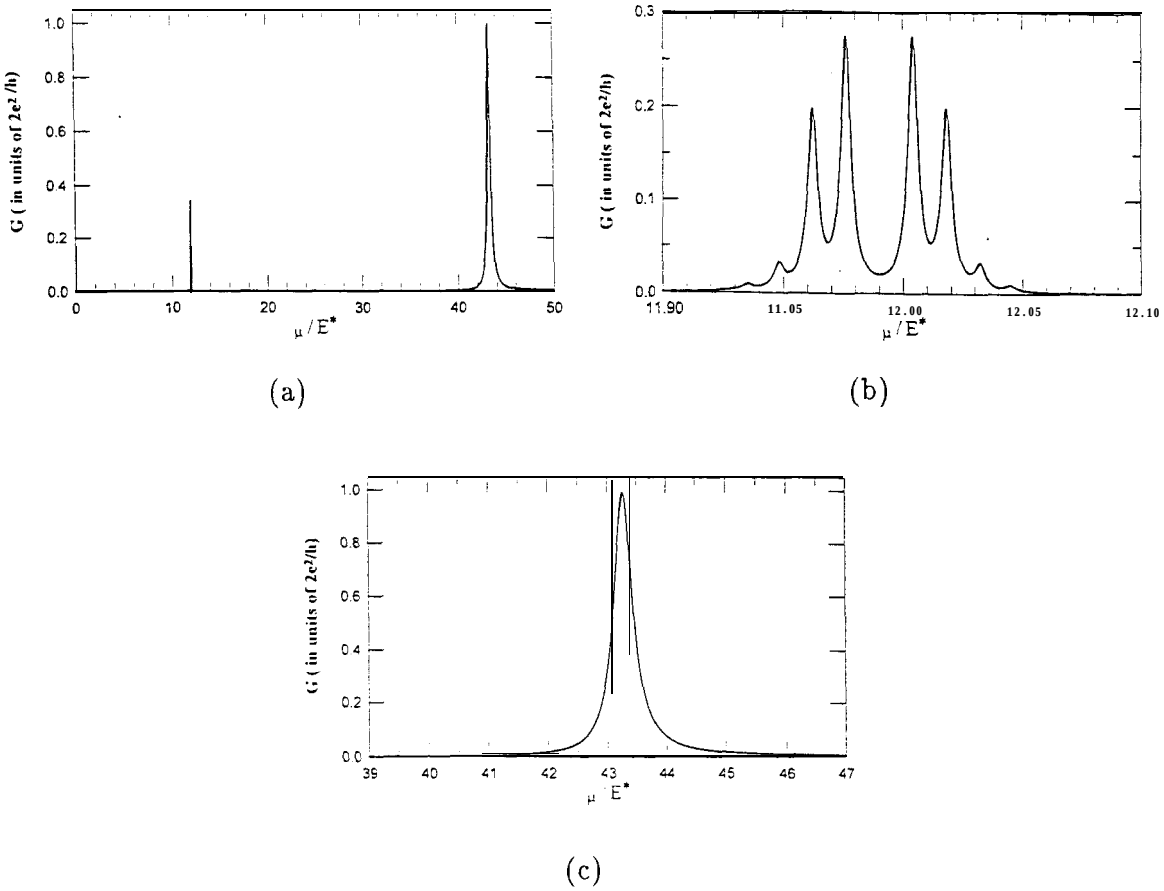

FIG. 5. Conductance G as a function of μ for a double-barrier structure acted upon by a time-modulated potential. Well width d = 50/79.6, L = 3d, barrier height $V_0 = 500/9$, and $\omega = 0.014$. V_1 = (a) 0.03, (b) 2.585ω, and (c) 2.585ω. In Fig. 5(a), V_1 is too small to induce observable photon-assisted transmission in the neighborhood of the resonant state $\mu = E_b^{e(o)}$. In Fig. 5(b), with a slightly larger V_1, the time-modulated potential gives rise to quenching effect near the first resonant state. This is consistent with the findings of Wagner. In Fig. 5(c), such quenching effect is not found near the second resonant state.

shows that the symmetry G(m) = G(-m) occurs at the actual location of the resonant level.

IV. Conclusion

We have solved nonperturbatively the quantum transport in a double-barrier structure in presence of a time-modulated potential. The scattering process is both coherent and inelastic. We extend quasi-bound features in all potential ranges and in all frequency

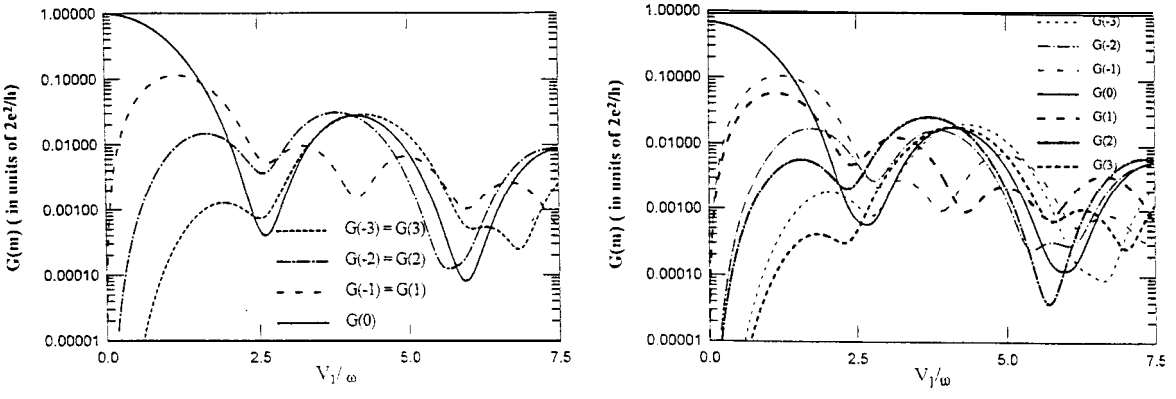

(a) (b)

FIG. 6. Conductance component G(m) as a function of V_1/ω for a double-barrier system. Well width d = 50/79.6, L = $3d$, barrier height V_0 = 500/9, w = 0.014, and V_1 = 2.585ω. In Fig. 6(a), at the peak of the resonant transmission, where μ = 11.99, we find that G(m) = G(-m). However, in Fig. 6(b), at $\mu = E_b$ = 11.992, G(m) is not equal to G(-m).

ranges. Two possible sets of structures in G can occur, either when $\mu = m\hbar\omega$ or when $\mu = E_b \pm m\hbar\omega$. The resonant level has to be sharp enough for the quenching effect to the resonant transmission to occur.

Acknowledgements

This work was partially supported by the National Science Council of the Republic of China through Contract No. NSC 88-2112-M-009-028.

References

[1] M. Büttiker and R. Landauer, Phys. Rev. Lett. 49, 1739 (1982).
[2] D. D. Coon and H. C. Liu, J. Appl. Phys. 58, 2230 (1985).
[3] X. P. Jiang, J. Phys. Condens. Matter 2, 6553 (1990).
[4] M. Y. Azbel, Phys. Rev. B43, 6847 (1991).
[5] P. F. Bagwell and R. K. Lake, Phys. Rev. B46, 15329 (1992).
[6] F. Rojas and E. Cota, J. Phys. Condens. Matter 5, 5159 (1993).
[7] M. Wagner, Phys. Rev. B49, 16544 (1994).
[8] M. Wagner, Phys. Rev. A51, 798 (1995)
[9] V. A. Chitta *et* al., J. Phys. Condens. Matter 6, 3945 (1994).
[10] L. Y. Gorelik *et al.*, Phys. Rev. Lett. 75, 1162 (1995).
[11] C. S. Tang and C. S. Chu, Phys. Rev. B53, 4838 (1996).
[12] C. S. Chu and H. C. Liang, to be published.